MUON SHIELDING CALCULATIONS: HETEROGENEOUS PASSIVE AND ACTIVE SHIELDS, APPLICATIONS TO EXPERIMENTAL BEAMS AND AREAS

D. Theriot, M. Awschalom and K. Lee

National Accelerator Laboratory *)
Batavia, Illinois 60510, U.S.A.

1. INTRODUCTION

With the advent of a new generation of high-energy and high-intensity proton accelerators such as the one being built at the National Accelerator Laboratory and the one proposed by CERN, the problem of shielding external proton targets, the secondary beams produced from these targets, and even the secondary targets in the experimental areas becomes quite a massive and expensive project. In addition to the massive hadron shielding required, the high-energy muons produced by the decay of pions and kaons add large amounts of shielding especially in the forward (beam) direction.

Homogeneous shields can be designed with programs which have been discussed previously[1]. We have developed a computer program which allows us to design heterogeneous shields with voids and/or magnetic fields. The heterogeneous shields without magnetic fields are called passive shields and those with magnetic fields are called active shields. Results of some of the studies made on the design of such shields are presented. Specific application to the design of shielding for a primary external proton beam target and for a specific experiment are discussed.

---

*) Operated by Universities Research Association, Inc., under contract with the U.S. Atomic Energy Commission.

2. CALCULATIONAL DETAILS

2.1 Muon source term

Protons from a 200-GeV beam interact in a target. These protons give rise to pions which have an energy-angle distribution corresponding to the differential production spectrum, $d^2N_\pi/dp_\pi d\Omega$ from proton-nucleus collisions. We take this pion production spectrum from the work of Trilling with constants adjusted to the latest values[2]. In drifting a distance Δ before striking a shield and interacting, some of these pions decay to muons traveling very close to the same direction as the parent pion. The probability for such a decay is given by $P(p_\pi,\Delta)=\Delta/\lambda p_\pi$ where p_π is the pion momentum, and λ is 55m $(GeV/c)^{-1}$. The decay of a pion of momentum p_π gives rise to a flat spectrum of muons with momenta between 0.57 p_π and p_π. The contribution from kaon decays is ignored in the present calculation. However, the program can be easily adapted to handle them. We are planning to introduce kaon decays in the near future when it will be necessary to estimate neutrino fluxes from muon fluxes in the neutrino laboratory.

In actual application we scan p_π between the beam momentum and a $p_{\pi min}$ generally chosen by consideration of the minimum momentum muon which can reach the location in the shielding we are interested in. The pion momenta are chosen uniformly between p_p and $p_{\pi min}$. A similar scan is made of θ, the polar angle of the pion. θ_{min} and θ_{max} can be chosen according to the needs of the particular problem being considered. In general, θ is not evenly spaced but is chosen biased toward the smaller production angles. Δ is calculated for each pion. If the target is in front of a shielding wall, Δ is the distance traveled before hitting the shielding wall. If the target is the front of the shield itself, Δ is 1.8 L_o where L_o is the nuclear absorption mean-free path in the shielding material[3].

Each pion generated from our scans is allowed to decay into several muons, the weight of each muon being reduced accordingly. The muon momentum is chosen randomly in the allowed kinematic range. It is assumed that the muon and pion momenta are collinear. After these muons are produced an azimuthal angle ϕ is chosen at random for each of them and the muon begins to be transported through the shielding.

2.2 Muon transport

Upon entering the shielding the muons begin to lose momentum through interactions and to multiple Coulomb scatter. The muon momentum loss per unit distance is a linear function of p_μ calculated by fitting values of an average dE/dx including losses due to atomic excitations and ionization, bremsstrahlung, pair production and nuclear interactions[4]. Different momentum loss rates are calculated for each different type of shielding material, and all range straggling is neglected. A simple Gaussian multiple Coulomb scattering formula is used. Corrections due to Moliere and any radiative effects are neglected.

If the muon enters a region where a magnetic field is present, it is deflected according to its charge and the direction of the magnetic field. Each component of the magnetic field is handled separately. At present we model magnets having only two components transverse to the initial proton direction.

An arc length is chosen for the transport of muons through each material. A muon incident upon a shield is carried one arc length according to its initial direction cosines and with its initial momentum. At the end of that arc length its momentum is decreased by the appropriate amount, its direction cosines are changed by choosing a scattering angle in a Monte Carlo fashion with the customary Gaussian distribution for multiple Coulomb scattering, and if a magnetic field is present the direction cosines

are changed again in the appropriate fashion. If a boundary in the shield is crossed or the momentum drops below zero in a given arc length, a step is taken backwards to that boundary or to zero momentum and all of the direction cosines are changed by smaller amounts by an interpolation routine. This process continues in transporting the muons throughout the shield. When a muon encounters a void in the shield, that muon is transported across the void in a single step without reducing its momentum or adding multiple Coulomb scattering. However, magnetic fields may exist and be effective in the void.

At various points throughout the shield, boundaries are drawn and various distributions are taken relating to the muons crossing that boundary. Flux, angular, and momentum distributions are common ones. Limits can also be applied, i.e., the distributions can be limited to those muons which cross a given area. These limits can be placed on either the distributions alone or the muons themselves, i.e., the limit can exclude a muon from being included in distributions at one boundary, but that same muon can contribute to distributions at subsequent boundaries or that muon can simply cease being transported because it did not fall within certain limits. These limit features allow one to ask detailed questions about muons at a particular spot in the shield or about muons that crossed a certain aperture.

3. RESULTS AND DISCUSSION

3.1 Comparison with R. G. Alsmiller's calculations

It has been mentioned earlier in the paper that muon shielding calculations for homogeneous shields have been previously discussed[1]. These calculations were performed by R. G. Alsmiller, Jr. of ORNL and are hereafter referred to as Alsmiller's calculations. Dr. Alsmiller has been kind enough to let us use his programs. Alsmiller's

calculations use the same Trilling production formulae and similar dE/dx equations as ours. Instead of applying multiple Coulomb scattering in a Monte Carlo fashion, his programs use the semi-analytical method of Eyges[5]. Range straggling is also neglected. Taken in all, these programs form a good bench mark to which we can compare our work.

The test case chosen for the comparison was that of earth shielding for muons created between the angles of 0 and 25 mrad by a beryllium target six meters in front of the shield. The comparison is shown in Fig. 1. The flux is shown in units of muons per square centimeter per interacting proton for five different depths in the shield as a function of radius. The solid lines represent Alsmiller's calculations and the dashed lines and points represent this work. Everywhere throughout this vast shield ranging through six orders of magnitude in flux we agree within a factor of two. There is a slight systematic shift from overprediction at small depths to underprediction at large depths but this can be explained by our simplistic approach to using a linear expression for dE/dx while Alsmiller uses a more accurate expression. In general, we feel that we are in agreement with Alsmiller's calculations. This gives us confidence in applying our program to the problem of heterogeneous shields with voids and magnetic fields which cannot be handled using the Eyges theory.

3.2 Design of a passive shield with voids

The first application which we will discuss is a study of the muon shielding required by a target in the primary proton beam of 10^{13}, 200 GeV protons interacting per second in a beryllium target. Surrounding the target is a void with a radius of 6 in. and a length of 20 ft. Surrounding this void is a steel box with lateral walls 2 ft thick and a wall in the downstream beam direction 20 ft thick. This steel target box is then embedded in a mass of earth which will form the main muon shielding. The result is shown

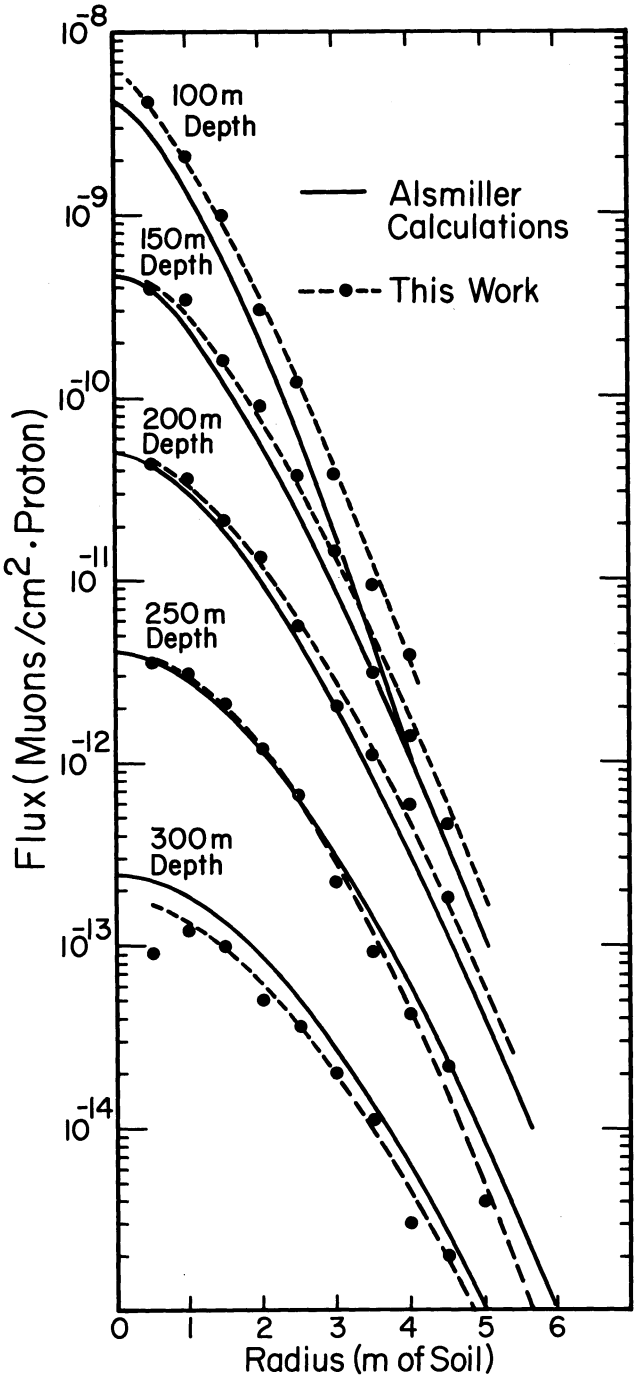

Fig. 1 A detailed comparison of Alsmiller's calculations with this work. Soil density is 2.0 gm/cm^3.

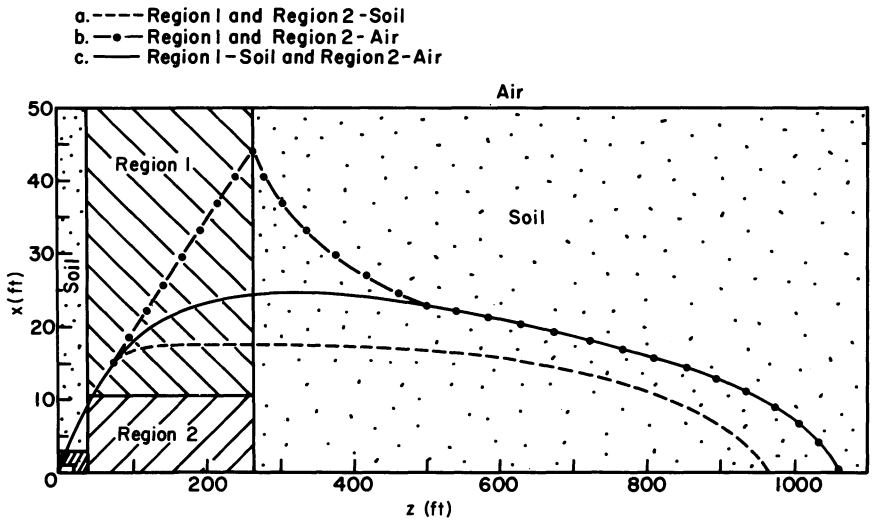

Fig. 2 A study of the effect of voids in earth shielding. Lines shown correspond to the 10^{-13} isoflux curve for each case.

as case (a) in Fig. 2.

The dashed curve is the 10^{-13} isoflux line. The units of an isoflux line are muons per square centimeter per interacting proton, i.e., for 10^{13} interacting protons, 1 muon per square centimeter would be present along this curve. The dimensions of the earth shield called for in this case was a radius of approximately 17 ft and a length of 960 ft.

Since this primary target was to be the source of several secondary beams, it was not possible to place the muon shield this close to the target. In actual practice the target will be surrounded by just enough shielding to attenuate the hadrons sufficiently. The beam transport front end will follow and then the main muon shield would begin. Just what changes this would produce in the shape and size of the muon backstop had to be considered.

As a first approximation we simply cut a slice out of the earth shield. In the regions 1 and 2 extending from z = 40 ft to z = 265 ft the earth was simply cut away and

replaced by air. The resulting 10^{-13} isoflux curve is shown as case (b) in Fig. 2. Note that the isoflux curve diverges quite rapidly in this region of air reaching a radial size of 45 ft at z = 265 ft where the earth shield begins. Once in the earth shield the radial size of the isoflux curve shrinks quite rapidly as the low energy muons are ranged out; however, it does not decrease to the size that it would have been if the cut had not been there. The typical increase in radial size between case (a) and case (b) is 6 to 7 ft except in the region near z = 265 ft where it is considerably larger. Note also the increase in the length of the shield to z = 1060 ft from the previous 960 ft.

The second approximation was to create an underground void 10.5 ft high, 225 ft long, and 20 ft wide which would house the front end beam transport but which would be covered with earth to avoid the necessity of creating earth berms 45 ft high. This had the practical advantage of also providing hadron shielding for the beam losses that would occur in these front end transport magnets. The results are shown as case (c) in Fig. 2. The high peak has now disappeared and the largest radial dimension required is now 25 ft instead of 45 ft. As z increases, cases (b) and (c) merge. The actual shield that was built to provide the muon backstop for this target has dimensions very close to that called for in case (c).

3.3 Design of an active shield with voids

We have applied our program to study the muon shielding required in an experiment that will produce a beam of hyperons. A 200-GeV proton beam of 10^{10} particles per second is incident upon a target followed immediately by a long, narrow magnetic channel. In the case of a neutral hyperon beam, this channel merely sweeps all charged particles out of the beam. In the case of a charged hyperon beam this channel disposes of oppositely charged particles

and of particles off the desired momentum. Downstream of the channel is a small experimental area and shielding to reduce the muon fluxes to tolerable levels.

We have chosen to investigate the behavior of the muons in the median plane of the magnetic channel and all areas downstream of it. The model chosen for our magnet is simple. The magnet is 20 ft long. In the central region from +6 to -6 inches there is a magnetic field of 10 kilogauss. On either side from 6 inches out to 12 inches is a return leg with a field of 10 kilogauss in the opposite direction. These dimensions were chosen to correspond to an NAL main ring magnet. The abrupt change in direction of the magnetic field takes place approximately three quarters of the way through the coil. A more complicated model could be drawn but we feel that this model is sufficient for our purposes.

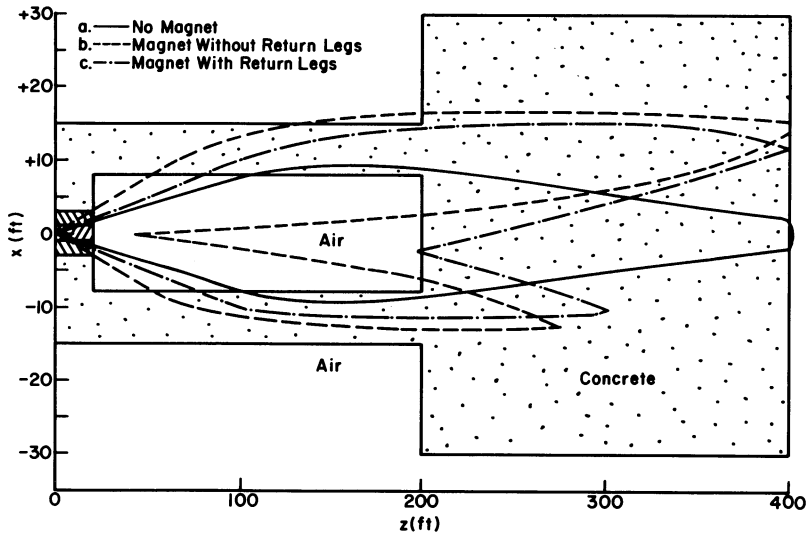

Fig. 3 A study of the effect of magnetic fields on heterogeneous shielding. Lines shown correspond to the 10^{-10} isoflux line in each case.

Some results are shown in Fig. 3. The general geometry of the area is indicated. The magnet and iron for the hadron dump occupy the region 0 to 20 ft. There is an experimental cave 180 ft long and 15 ft wide with ordinary

concrete shielding on either side and at the back. The shielding array fed into the program is shown. It is overly generous and the purpose of the program is to show us how much we can cut it. The first case tested was with the magnet turned off. The 10^{-10} isoflux line is shown as a solid curve. This is the shielding required when the magnet is turned off. The next case tested was the non-physical one of using the central magnetic field only with no return legs. The results for the 10^{-10} isoflux line are shown as the dashed curve. Notice that the muons are separated into two beams each corresponding to one charge and that there is a gap between the two beams where the muon flux is quite low. Furthermore, the upper beam of positive muons is of higher intensity than the lower beam of negative muons as indicated by the amount of shielding required to attenuate them to this level. When the return legs are added to the magnetic field, those low energy muons which were swept out by the central field are now swept back toward the center line by the return legs. The result for the 10^{-10} isoflux is shown by the dot-dash line. Note that the nice low flux hole that existed in case (b) has now disappeared and the entire experimental area is bathed in a sea of muons. These low energy muons that have been swept back by the return legs could be attenuated by the addition of passive iron shielding immediately down-stream of the magnet and the low flux area can be recovered if it is desirable to have such a place in which to locate experimental apparatus.

Shown in Fig. 4 is a set of isoflux curves for case (c), the magnet with return legs. The design intensity of the diffracted proton beam at NAL is 10^{10} protons/sec. We design our shields nominally for 1 muon/(cm^2.sec), allowing for various uncertainties in pion production and muon attenuation. Using this criterion we would build a shield corresponding to the 10^{-10} isoflux line, taking care to

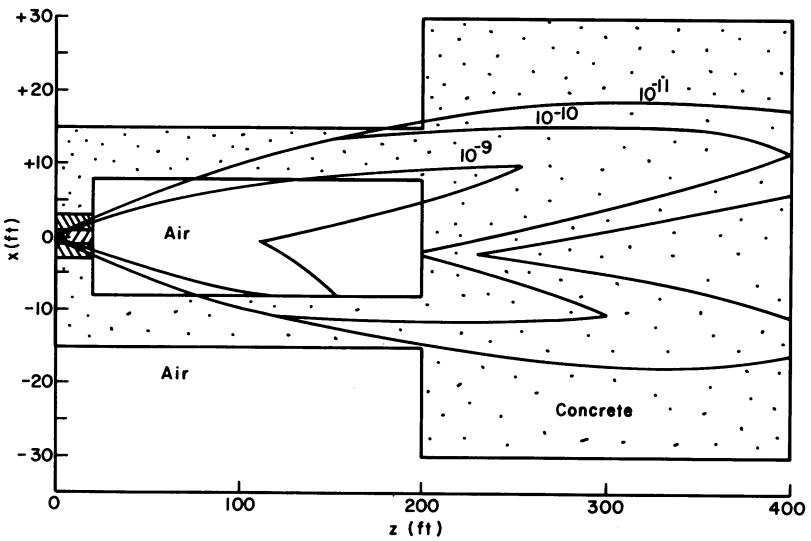

Fig. 4 Isoflux curves for case (c) of Fig. 3. Units shown are muons/(cm^2.int.proton).

include the case (a) with the magnet turned off in our arrangement of shielding blocks.

4. CONCLUSION

The two examples discussed show that this computer program is versatile and that it can be used in the actual geometries encountered in radiation safety work. At this stage we must admit that everything in this paper is theoretical. No part of it has stood the test of an experiment. However, by the end of this year we hope to have data on muon shielding from 200-GeV proton interactions. Then, we shall be able to check the accuracy of the source term as well as the transport part of the program.

REFERENCES

1) R. G. Alsmiller, Jr., M. Leimdorfer and J. Barish, ORNL-4322 (1968).

2) J. Ranft and T. Borak, NAL-FN-193 (1969).

3) D. Keefe and C. M. Noble, UCRL-18117 (1968).

4) D. Theriot, NAL-TM-229 (1970).

5) L. Eyges, Phys. Rev. 74, 1534 (1948).